Available online at www.sciencedirect.com
SCIENCE DIRECT®
Journal of Solid State Chemistry 176 (2003) 192–197
JOURNAL OF SOLID STATE CHEMISTRY
http://elsevier.com/locate/jssc

Preparation, crystal structure, and magnetic studies of $Na_3Fe_2Mo_5O_{16}$, a new oxide containing Mo_3O_{13} clusters

K.G. Bramnik,* E. Muessig, and H. Ehrenberg

Institute for Materials Science, Darmstadt University of Technology, Petersenstr. 23, Darmstadt D-64287, Germany

Received 28 April 2003; received in revised form 10 June 2003; accepted 14 July 2003

Abstract

The complex oxide $Na_3Fe_2Mo_5O_{16}$ has been synthesized, and its crystal structure was determined by single-crystal X-ray diffraction (space group (SG) $P\text{-}3m1$; $a = 5.7366(6)$ Å, $c = 22.038(3)$ Å; $Z = 2$). The compound can be considered as a new structure type containing Mo_3O_{13} cluster units, which can be derived from the $Na_2In_2Mo_5O_{16}$ structure model by doubling of the cell along the c-axis. $Na_3Fe_2Mo_5O_{16}$ crystallizes in centrosymmetric SG ($P\text{-}3m1$) and the positions of the sodium atoms are fully occupied in contrast to the proposed $Na_2In_2Mo_5O_{16}$ model SG ($P3m1$). Magnetic properties of $Na_3Fe_2Mo_5O_{16}$ were studied by superconducting quantum interference device measurements, revealing antiferromagnetic ordering below $T\chi_{max} = 10(1)$ K. Thermal stability in air was investigated by in situ high-temperature X-ray powder diffraction. Structural relationships to $Na_2In_2Mo_5O_{16}$ and $NaFe(MoO_4)_2$ are discussed.

Keywords: Mo_3O_{13} cluster; Metal bond; Antiferromagnetic ordering; Layered compound; Structure solution

1. Introduction

Several different structure types with Mo_3O_{13} clusters have been reported in literature [1–8]. These cluster units consist of three triangular-forming edge-sharing MoO_6 octahedra, held together by three one-fold metal–metal bonds. Two different connectivity schemes between Mo_3O_{13} cluster units are described in literature: in $La_3Mo_4SiO_{14}$ [1,2] infinite linear chains are built by edge sharing. In the other known structures, Mo_3O_{13} units are linked by sharing of two common edges. It results in infinite layers in the *ab*-plane with Mo_3O_8 layer composition [2–9]. Mo_3O_8 sheets can be separated from each other in different ways reflected in the variation of the unit-cell parameter perpendicular to the Mo_3O_8 planes. $LiRMo_3O_8$ (with R= Sc, Y, In, Sm, Gd, Yb, Lu) [3,4] compounds ($c = 4.94-5.27$ Å) adopt a structure with only one Mo_3O_8 layer per unit cell separated by lithium and rare-earth atoms in tetrahedral and octahedral interstices, respectively. $M_2Mo_3O_8$ (M= Mg, Mn, Fe, Co, Ni, Zn, Cd) include two Mo_3O_{13} sheets per unit cell, separated by layers of M atoms, again situated in octahedral and tetrahedral interstices. The alternating sequence of the filled tetrahedral and octahedral sites along [001] direction results in a doubling of the unit cell ($c = 9.87-10.82$ Å) [5]. $LiZn_2Mo_3O_8$ and $Zn_3Mo_3O_8$ [6] belong to another structure type, derived from the $M_2Mo_3O_8$ cell by a three-fold cell parameter c ($c = 31.01-31.10$ Å). This is the result of an additional zinc site between the Mo_3O_8 layers, so that additional layers with filled tetrahedral and strongly distorted octahedral coordination exist. In $Li_4Mo_3O_8$ with cell parameters close to $LiZn_2Mo_3O_8$, one-quarter of the lithium atoms fill octahedral interstices inside the Mo_3O_8 layers [7]. These layers are separated from each other in the same way as in the $M_2Mo_3O_8$ structure, but with all tetrahedral positions occupied. Therefore, this compound is better described as $Li_3(LiMo_3O_8)$. Another arrangement of the cations in between Mo_3O_8 layers is reported in literature for $Na_2In_2Mo_5O_{16}$ [8]: Mo_3O_8 layers are separated from each other by ~ 11.27 Å along [001] direction, this distance corresponds to the cell parameter c. These sheets are connected by a network of InO_6 octahedra and MoO_4 tetrahedra with Na atoms occupying large cavities in this network. The compound, $LaMo_2O_5$, [9] represents an exception from structure types with

*Corresponding author. Fax: +49-6151-166377.
E-mail address: bramnik@tu-darmstadt.de (K.G. Bramnik).

0022-4596/$ - see front matter © 2003 Elsevier Inc. All rights reserved.
doi:10.1016/S0022-4596(03)00390-6

Table 1
Details of single-crystal X-ray data collection and structure refinement of $Na_3Fe_2Mo_5O_{16}$

Empirical formula	$Na_3Fe_2Mo_5O_{16}$
Formula weight	916.37 g/mol
Temperature	293(2) K
Wavelength	0.71073 Å(Mo$K\alpha$)
Space group	P-3m1 (no. 164)
Unit-cell dimensions	$a = 5.7366(6)$ Å, $c = 22.038(3)$ Å, $V = 628.06(12)$ Å^3
Z	2
Calculated density (g/cm^3)	4.846
Absorption coefficient	7.276 mm^{-1}
F (000)	846
Crystal shape and size	Platelets, $0.09 \times 0.05 \times 0.02$ mm^3
θ range for data collection	2.77–29.86°
Limiting indices	$-7 \leqslant h \leqslant 7$, $-7 \leqslant k \leqslant 7$, $-30 \leqslant l \leqslant 27$
Reflections collected/unique	2796/738, $R_{int} = 3.84\%$
Completeness to $\theta = 29.86$	95.3%
Refinement method	Full-matrix least squares on F^2
Data/restrains/parameters	738/0/59
Final R indices ($I > 2\sigma$)	$R_1 = 4.75\%$, w$R_2 = 13.29\%$
R indices (all data)	$R_1 = 6.26\%$, w$R_2 = 15.12\%$
Largest difference peak and hole	1.820 and $-2.060e$ Å^{-3}

Mo_3O_{13} cluster units: Its structure contains both isolated Mo_6O_{18} clusters and sheets of fused triangular Mo_3 clusters.

In the present contribution we describe the synthesis, crystal structure, thermal stability, and magnetic properties of the new compound, $Na_3Fe_2Mo_5O_{16}$, with Mo_3O_{13} cluster units.

2. Experimental

Na_2MoO_4 (Aldrich, 99%), Fe_2O_3 (Aldrich, 99.98%), and MoO_2 (STREM Chemicals, 99%) were chosen as starting materials. Stoichiometric amounts of the reagents were intimately mixed, ground in an agate mortar and placed in an alumina crucible to avoid a reaction with the silica tube during annealing. This sample was sealed in a silica tube with a 8–10 cm^3 volume at 10^{-3} mbar pressure. The raw material was annealed for 48 h at 700°C, afterwards cooled down to the room temperature in the furnace.

Black plate-like-shaped crystals were obtained after the synthesis. The crystal structure was solved by single-crystal X-ray diffraction data analysis using the Xcalibur system from Oxford Diffraction. Details of data collection and structure refinement are summarized in Table 1. The software package SHELXS [10] and SHELXL [11] were used for structure solution and refinement, respectively, as included in X-STEP32 [12].

X-ray powder diffraction data were collected with a STOE STADI/P powder diffractometer (Mo$K\alpha_1$ radiation, curved Ge monochromator, transmission mode, step 0.02°(2θ), linear PSD counter) for phase analysis and crystal structure confirmation. The Winplotr package [13] was used for structure refinements based on powder data.

The magnetic properties of $Na_3Fe_2Mo_5O_{16}$ were studied using a superconducting quantum interference device from Quantum Design in the temperature range from 4.5 to 300 K with an applied field strength of 0.05 T.

High-temperature X-ray powder diffraction data were collected in air with a STOE STADI/P powder diffractometer (Mo$K\alpha_1$ radiation, curved Ge monochromator, Debye–Scherrer mode, image-plate detector) in the temperature range from 125°C to 625°C.

3. Results and discussion

3.1. Structure determination

The structure solution of $Na_3Fe_2Mo_5O_{16}$ revealed a new structure containing Mo_3O_{13} cluster units. Positional parameters and selected interatomic distances are listed in Tables 2 and 3, respectively. The X-ray powder diffraction pattern of an annealed sample with a $Na_3Fe_2Mo_5O_{16}$ bulk composition was almost completely indexed on the basis of a primitive hexagonal cell with $a = 5.7366(6)$ Å, $c = 22.038(3)$Å. The presence of a small amount of an unknown admixture (the strongest reflex of admixture has less than 6% intensity of the strongest reflex of the main phase) could be established. A single-phase powder could be achieved after washing the sample in 70% HNO_3.

The crystal structure of $Na_3Fe_2Mo_5O_{16}$ is closely related to the already known $Na_2In_2Mo_5O_{16}$ [8]. The main structure units in these compounds are infinite sheets of edge-shared MoO_6 octahedra in ab-plane with Mo_3O_8 composition. The described sheets can also be considered as a hexagonal close packing of oxygen atoms, where molybdenum atoms fill octahedral cavities in such a way that in each second row along a- or b-direction the filled cavities alternate with vacant octahedral position. Projection of this layer along [001] is schematically shown in Fig. 1. Mo atoms are connected by one-fold metal–metal bonds within each layer. The Mo–Mo bond distance, 2.567(1) Å, is significantly shorter than in metallic Mo, 2.726 Å, and fits to metal–metal bond lengths in other compounds containing Mo_3O_{13} metal cluster units, see Table 4. The metal–metal distances in these structures correlate with the number of electrons per Mo_3O_{13} cluster unit and increase with decreasing formal oxidation state of Mo in the Mo_3O_8 sheets. The same effect of Mo–Mo bond elongation was observed for isolated Mo_3O_{13} clusters: 2.486(1) Å for Mo^{+4} in $Cs_2[Mo_3O_4(C_2O_4)_3(H_2O)_3] \cdot 4H_2O \cdot \frac{1}{2}H_2C_2O_4$ [19] and 2.550(2) Å for Mo_{+35} in

Table 2
Positional and thermal displacement parameters for $Na_3Fe_2Mo_5O_{16}$

Atom	Wyck.	x/a	y/b	z/c	U_{eq} (Å^2)
Mo(1)	2*d*	2/3	1/3	0.56780(8)	0.004(1)
Mo(2)	2*d*	2/3	1/3	0.06459(8)	0.005(1)
Mo(3)	6*i*	0.4825(1)	0.9650(2)	0.25603(4)	0.003(1)
Fe(1)	2*c*	0	0	0.6480(1)	0.004(1)
Fe(2)	2*c*	0	0	0.1486(1)	0.005(1)
Na(1)	1*a*	0	0	0	0.023(3)
Na(2)	1*b*	0	0	1/2	0.014(3)
Na(3)	2*d*	2/3	1/3	0.3871(4)	0.018(2)
Na(4)	2*d*	2/3	1/3	0.8837(4)	0.024(2)
O(1)	2*d*	2/3	1/3	0.4900(7)	0.012(3)
O(2)	2*d*	2/3	1/3	0.6801(6)	0.002(3)
O(3)	6*i*	0.6662(15)	0.8331(8)	0.6953(4)	0.003(2)
O(4)	6*i*	0.3364(16)	0.1682(8)	0.7992(4)	0.005(2)
O(5)	2*d*	2/3	1/3	0.9861(8)	0.017(4)
O(6)	2*d*	2/3	1/3	0.2097(7)	0.005(3)
O(7)	6*i*	0.8417(9)	0.1583(9)	0.5853(4)	0.012(2)
O(8)	6*i*	0.8362(9)	0.1638(9)	0.0891(4)	0.019(2)

Table 3
Characteristic interatomic distances (Å) for $Na_3Fe_2Mo_5O_{16}$

Mo(1)–O(1)	1.715(16)	Mo(2)–O(5)	1.730(18)
O(7)	1.781(6)	O(8)	1.769(7)
O(7)	1.782(2) × 2	O(8)	1.769(3) × 2
Mo(3)–Mo(3)	2.567(1) × 2		
Mo(3)–O(2)	2.044(9)	Fe(1)–O(3)	1.959(8) × 3
O(3)	2.051(5) × 2	O(7)	2.094(6) × 3
O(4)	1.985(9) × 2	Fe(2)–O(4)	2.029(8) × 3
O(6)	2.095(8)	O(8)	2.090(6) × 3
Na(1)–O(8)	2.550(7) × 6	Na(2)–O(7)	2.451(7) × 6
Na(3)–O(1)	2.268(18)	Na(4)–O(4)	2.48(1) × 3
O(3)	2.46(1) × 3	O(5)	2.26(2)

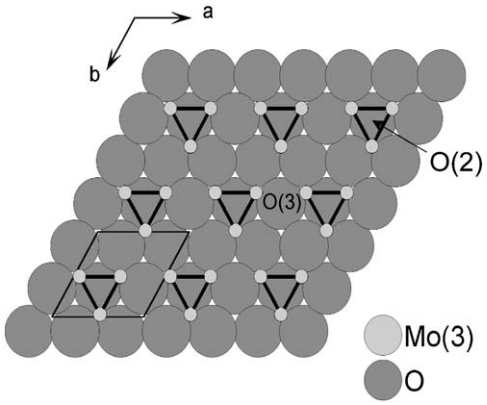

Fig. 1. The filling scheme of octahedral cavities by Mo atoms within Mo_3O_8 layers.

$[Mo_3OCl_3(O_2CCH_3)_3(H_2O)_3](ClO_4)Cl$ [20]. The LCAO–MO calculations for an ideal isolated Mo_3O_{13} cluster explained this tendency [21] taking into account the following electron distribution: six electrons of the Mo_3O_{13} cluster (two electrons from each Mo^{+4}) occupy strong bonding molecular orbitals (a_1 and e), while the next electron would occupy a relative non-bonding orbital. More recent *MO* calculations of $[Mo_3O_4]^{4+}$ and $[Mo_3O_4(OH)_6(H_2O)_3]^{2-}$ [22] have shown a great influence of capping and edge-bridged oxygen atoms of the $[Mo_3O_4]^{4+}$ core on the Mo–Mo bonding interaction. Two different reasons for the metal–metal bond elongation were suggested: (1) the reduction of effective metal charge from +4 to $+3\frac{1}{3}$, which should be accompanied by an increase in the effective atomic radius of the Mo atoms, or (2) the increase of electron donation from the ligands into a weak antibonding orbital of Mo_3^{10+}. (The third proposed explanation based on the replacement of one oxygen atom by a larger Cl atom in the $[Mo_3O_4]$ core is irrelevant for our consideration.) The first proposed mechanism and a possible influence of neighboring atoms on Mo–O π bonding was discussed in detail for the cases of $Zn_2Mo_3O_8$, $LiZn_2Mo_3O_8$, and $Zn_3Mo_3O_8$ (six, seven, and eight electrons per Mo_3O_{13} cluster) [6].

Deviation from this rule in the case of $Mn_2Mo_3O_8$ can be easily explained as the result of comparatively high standard uncertainty in the observed bond distances. The partial substitution of Mo atoms within the Mo_3O_{13} cluster by Li atoms in $Li_4Mo_3O_8$ can lead to lengthening of the average metal–metal distance as in Li_2MoO_3 compound, 2.585 Å, where 10% of Mo sites are occupied by Li atoms [7]. An unexpected long Mo–Mo bond length, 2.6164(5) Å, was observed in $Na_2In_2Mo_5O_{16}$ [8]. Together with the proposed non-centrosymmetrical space group (SG) and vacancies in the Na(2) and Na(3) sublattices indicate that the correct unit cell of $Na_2In_2Mo_5O_{16}$ is doubled in *c*-direction with SG $P-3m1$ and all Na sites are fully occupied. Such a model would lead to an $Na_3In_2Mo_5O_{16}$ stoichiometry

Table 4
Structural data for compounds with Mo_3O_{13} units

Compound	Space group	Formal oxidation state of Mo in Mo_3O_8 sheet	d(Mo − Mo) Å	Reference
H_2MoO_3	Unknown	+4	2.506(1)[a]	[14]
$LiScMo_3O_8$	$P3m1$	+4	2.520(3)	[3]
$Zn_2Mo_3O_8$	$P6_3mc$	+4	2.524(2)	[15]
$LiInMo_3O_8$	$P3m1$	+4	2.525(3)	[4]
$Fe_2Mo_3O_8$	$P6_3mc$	+4	2.5296(6)	[16]
$Mg_2Mo_3O_8$	$P6_3mc$	+4	2.535(1)	[17]
$Co_2Mo_3O_8$	$P6_3mc$	+4	2.54(1)	[18]
$ScZnMo_3O_8$	$P6_3mc$	$+3\frac{2}{3}$	2.544(1)	[6]
$LiYMo_3O_8$	$P3m1$	+4	2.546(3)	[3]
$La_3Mo_4XO_{14}$ (X = Si, $Mo_{1/3}Al_{1/2}$, $Al_{1/2}V_{1/2}$)	$Pnma$	—[b]	2.550(1)–2.562(1)	[1,2]
$Mn_2Mo_3O_8$	$P6_3mc$	+4	2.56(4)	[18]
$Li_4Mo_3O_8$	R-3m	+4	2.560(1)	[7]
$Na_3Fe_2Mo_5O_{16}$	P-3$m1$	$+3\frac{2}{3}$	2.567(1)	This work
$LiZn_2Mo_3O_8$	R-3m	$+3\frac{2}{3}$	2.578(1)	[6]
$Zn_3Mo_3O_8$	R-3m	$+3\frac{1}{3}$	2.580(2)	[6]
$Na_2In_2Mo_5O_{16}$	$P3m1$	+4	2.6164(5)	[8]
$LaMo_2O_5$	$P6_3/mmc$	—[c]	2.612(9)–2.621(8)	[9]

[a] Data based on EXAFS study.
[b] The structures comprise chains of Mo_3O_{13} clusters interconnected with chains of Mo_2O_{10} clusters.
[c] The structure contains interconnected Mo_3O_{13} and Mo_6O_{18} clusters.

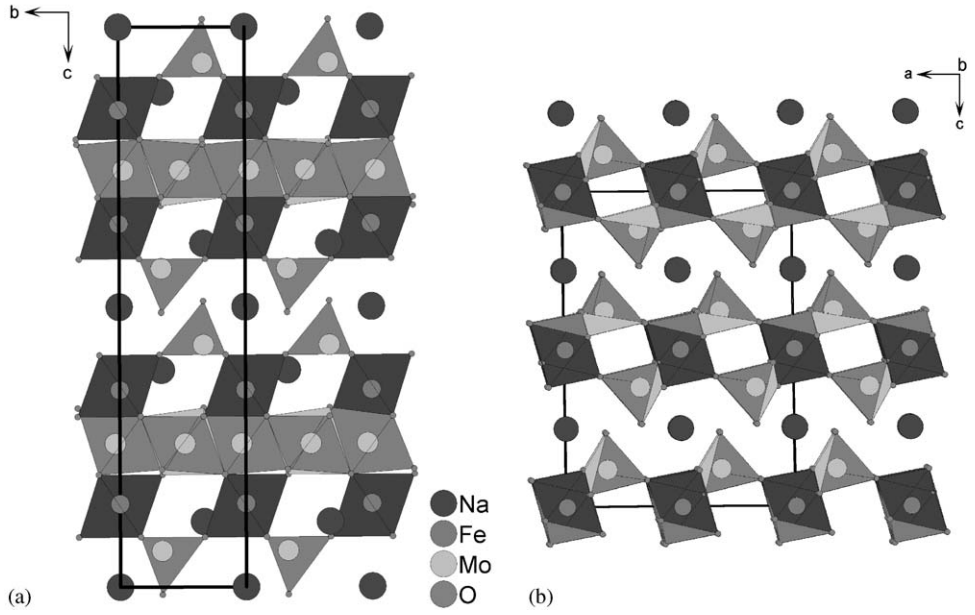

Fig. 2. The projections of (a) $Na_3Fe_2Mo_5O_{16}$ along the [100] axis and (b) $NaFe(MoO_4)_2$ along the [010] axis.

and, consequently, to a $+3\frac{2}{3}$ formal oxidation state of Mo within the Mo_3O_8 layers. The observed metal–metal bond length supports this consideration, it is still longer but more consistent with the lower formal oxidation state of Mo. The projection of the $Na_3Fe_2Mo_5O_{16}$ crystal structure along the [100] direction is shown in Fig. 2. The Mo_3O_8 layers are separated from each other by three close-packed layers of oxygen atoms partially replaced by Na atoms. Each second octahedral interstitial along the a- and b-axis of the nearest layer to an Mo_3O_8 sheet is filled by iron atoms, so that one-quarter of all octahedral interstitials in these layers are occupied. Molybdenum atoms fill tetrahedral interstices in the next oxygen layers in the same way. Therefore, the sum formula $Na_3Fe_2(MoO_4)_2Mo_3O_8$ takes the structure better into account. The sodium atoms, Na(1) and Na(2), have slightly distorted octahedral coordination with two non-equivalent distances d(Na−O) = 2.551

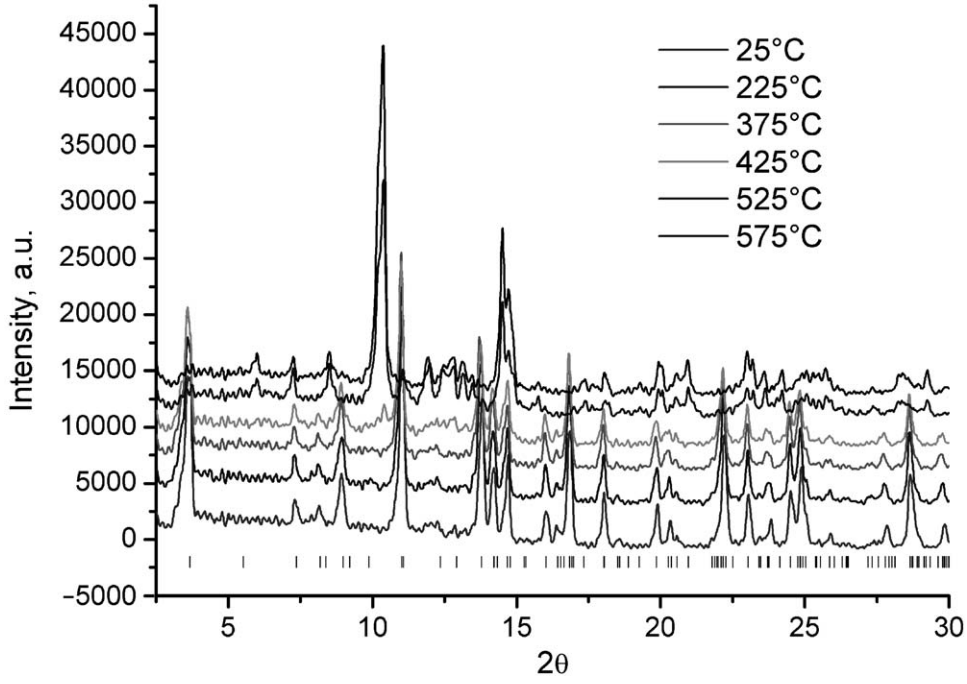

Fig. 3. X-ray powder diffraction patterns of $Na_3Fe_2Mo_5O_{16}$ at different temperatures in air.

and 2.450 Å, respectively, for two symmetry non-equivalent Na atoms. Other Na atoms, Na(3) and Na(4), are situated in strongly distorted oxygen tetrahedra. The average Na–O distances are 2.425 and 2.413 Å for Na(3) and Na(4), respectively. These bond lengths are in a very good agreement with the ionic radii of Na^+ for both tetrahedral and octahedral coordination as reported by Shannon [23]. In accordance with the average molybdenum–oxygen distance in the tetrahedral coordination, 1.766 Å for Mo(1) and 1.759 Å for Mo(2), to ionic radii [23] and to the same distances found in $Na_2In_2Mo_5O_{16}$ [8], one can conclude that the formal oxidation state of these Mo atoms is +6. The formal oxidation state +3 of Fe ions in $Na_3Fe_2(MoO_4)_2Mo_3O_8$ is consistent with the ionic radius of Fe^{3+} in a high-spin state with octahedral coordination.

Alternatively, the $Na_3Fe_2Mo_5O_{16}$ structure can also be considered as a coherent intergrowth of the $M_2Mo_3O_8$ and $NaFe(MoO_4)_2$ [24] structure motifs. The relationships between both structures are illustrated in Fig 2. Accordingly, the $Na_3Fe_2Mo_5O_{16}$ structure can be derived from $NaFe(MoO_4)_2$ by replacement of one MoO_4 layer by Mo_3O_8 sheets and filling the vacancies in close-packed oxygen layers by sodium atoms.

3.2. Thermal stability of the $Na_3Fe_2Mo_5O_{16}$

The thermal stability of $Na_3Fe_2Mo_5O_{16}$ in air was studied by high-temperature X-ray powder diffraction. As shown in Fig. 3, $Na_3Fe_2Mo_5O_{16}$ remains stable up to 375°C. With increasing temperature to 425°C, reflections of $NaFe(MoO_4)_2$ and $Na_2Mo_2O_7$ appear. Further increasing of temperature to 525°C leads to a complete oxidation and decomposition of the titled compound into a two-phase mixture of $NaFe(MoO_4)_2$ and $Na_2Mo_2O_7$ in ratio 2:1 (weight fractions defined from Rietveld refinement: 68(1)% and 32(1)%, respectively). This result is in a good agreement with a proposed decomposition reaction

$$4Na_3Fe_2Mo_5O_{16}+7O_2= 8NaFe(MoO_4)_2+2Na_2Mo_2O_7.$$

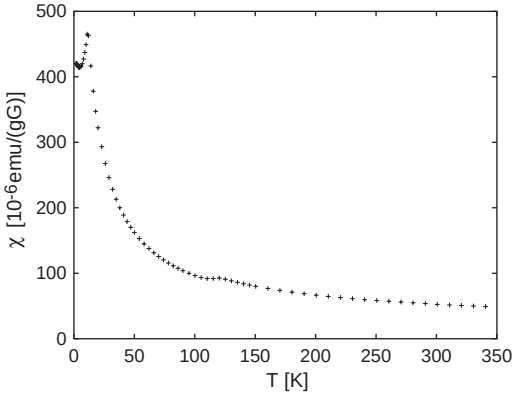

Fig. 4. Temperature dependence of magnetic susceptibility of $Na_3Fe_2Mo_5O_{16}$.

3.3. Magnetic properties of $Na_3Fe_2Mo_5O_{16}$

Temperature dependence of magnetic susceptibility obeys a modified Curie–Weiss law, $\chi(T) = C/(T-\Theta) +$

χ_0, with $\theta = -10$ K. A magnetic moment of 11.8(2) μ_B per formula unit was calculated from the Curie constant C, mainly due to the contributions from Fe ions in a $^6S_{5/2}$ state (theoretical value 5.92 μ_B per Fe ion). Therefore, small contributions from Mo ions can be neglected. A significant anomaly in the temperature dependence of the magnetic susceptibility is observed at 120 K, measured on two samples from different syntheses. A similar effect was also observed for $Na_2In_2Mo_5O_{16}$ [8] and might indicate a phase transition. Antiferromagnetic ordering is concluded from the pronounced maximum in $\chi(T)$ at $T = 10(1)$ K. The temperature dependence of magnetic susceptibility is shown in Fig. 4.

Acknowledgments

The authors thank Prof. Dr. H. Fuess for valuable discussions. Financial support by the Fonds der Chemischen Industrie is gratefully acknowledged.

References

[1] P.W. Betteridge, A.K. Cheetham, J.A.K. Howard, G. Jakubicki, W.H. McCarroll, Inorg. Chem. 23 (1984) 737–740.
[2] W.H. McCarroll, K. Podejko, A.K. Cheetham, D.M. Thomas, F.J. DiSalvo, J. Solid State Chem. 62 (1986) 241–252.
[3] J. DeBenedittis, L. Katz, Inorg. Chem. 4 (1965) 1836–1839.
[4] W.H. McCarroll, Inorg. Chem. 16 (1977) 3351–3353.
[5] W.H. McCarroll, L. Katz, R. Ward, J. Am. Chem. Soc. 79 (1957) 5410–5414.
[6] C.C. Torardi, R.E. McCarley, Inorg. Chem. 24 (1985) 476–481.
[7] S.J. Hibble, I.D. Fawcett, A.C. Hannon, Acta Crystallogr. B 53 (1997) 604–612.
[8] B.T. Collins, S.M. Fine, J.A. Potenza, P.P. Tsai, M. Greenblatt, Inorg. Chem. 28 (1989) 2444–2447.
[9] S.J. Hibble, S.P. Cooper, A.C. Hannon, S. Patat, W.H. McCarroll, Inorg. Chem. 37 (1998) 6839–6846.
[10] G.M. Sheldrick, Acta Crystallogr. A 46 (1990) 467–473.
[11] G.M. Sheldrick, SHELXL'97, Program for the Refinement of Crystal Structures, University of Göttingen, Germany.
[12] X-STEP32, STOE & Cie GmbH, Darmstadt, 2000.
[13] J. Rodriguez-Carvajal, Abstracts of the Satellite Meeting of the XV Congress of the International Union of Crystallography, Toulouse, 1995, p. 127.
[14] S.J. Hibble, I.D. Fawcett, Inorg. Chem. 34 (1995) 500–508.
[15] G.B. Ansel, L. Katz, Acta Crystallogr. 21 (1966) 482–485.
[16] Y. Le Page, P. Strobel, Acta Crystallogr. B 38 (1982) 1265–1267.
[17] R. Knorr, U. Mueller, Z. Anorg. Allg. Chem. 621 (1995) 541–545.
[18] D. Bertrand, H. Kerner-Czeskleba, J. Phys. 36 (1975) 379–390.
[19] A. Bino, F.A. Cotton, Z. Dori, J. Am. Chem. Soc. 100 (1978) 5252–5253.
[20] A. Bino, F.A. Cotton, Z. Dori, Inorg. Chim. Acta 33 (1979) L133–L134.
[21] F.A. Cotton, Inorg. Chem. 3 (1964) 1217–1220.
[22] B.E. Bursten, F.A. Cotton, M.B. Hall, R.C. Najjar, Inorg. Chem. 21 (1982) 302–307.
[23] R.D. Shannon, C.T. Prewitt, Acta Crystallogr. B 25 (1969) 925–946.
[24] R.F. Klevtsova, Dokl. Akad. Nauk SSSR 225 (1975) 1322–1325.